Journal of ELECTRONIC MATERIALS, Vol. 47, No. 2, 2018
DOI: 10.1007/s11664-017-5938-2
© 2017 The Minerals, Metals & Materials Society

TOPICAL COLLECTION: 59TH ELECTRONIC MATERIALS CONFERENCE 2017

DLTS Analysis and Interface Engineering of Solution Route Fabricated Zirconia Based MIS Devices Using Plasma Treatment

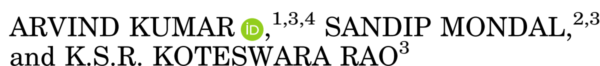
ARVIND KUMAR,[1,3,4] SANDIP MONDAL,[2,3] and K.S.R. KOTESWARA RAO[3]

1.—Department of Physics, Indira Gandhi National Tribal University, Amarkantak, Madhya Pradesh 484887, India. 2.—Department of Physics, Achhruram Memorial College, Purulia, West Bengal 723202, India. 3.—Department of Physics, Indian Institute of Science, Bangalore, Karnataka 560012, India. 4.—e-mail: arvind@igntu.ac.in

In this work, we have fabricated low-temperature sol–gel spin-coated and oxygen (O_2) plasma treated ZrO_2 thin film-based metal–insulator–semiconductor devices. To understand the impact of plasma treatment on the Si/ZrO_2 interface, deep level transient spectroscopy measurements were performed. It is reported that the interface state density (D_{it}) comes down to 7.1×10^{10} eV^{-1} cm^{-2} from 4×10^{11} eV^{-1} cm^{-2}, after plasma treatment. The reduction in D_{it} is around five times and can be attributed to the passivation of oxygen vacancies near the Si/ZrO_2 interface, as they try to relocate near the interface. The energy level position (E_T) of interfacial traps is estimated to be 0.36 eV below the conduction band edge. The untreated ZrO_2 film displayed poor leakage behavior due to the presence of several traps within the film and at the interface; O_2 plasma treated films show improved leakage current density as they have been reduced from 5.4×10^{-8} A/cm^2 to 1.98×10^{-9} A/cm^2 for gate injection mode and 6.4×10^{-8} A/cm^2 to 6.3×10^{-10} A/cm^2 for substrate injection mode at 1 V. Hence, we suggest that plasma treatment might be useful in future device fabrication technology.

Key words: Interface, DLTS, MIS, defect, thin film, plasma treatment

INTRODUCTION

The design of high permittivity (high-κ) gate dielectrics and channel layers for the thin film transistors (TFT) via wet chemical methods has garnered major interest, owing to the cost-effectiveness of the approach to produce the thin films with tailed structure-electronic properties.[1–3] Recently, ZrO_2 dielectric layers have shown the potential application in TFTs and sensors with high mobility channel layers.[4] High-temperature annealing is usually required to improve the electrical capacities of such thin films.[5] The interfacial layer (SiO_x) formation becomes significant at elevated temperatures during the deposition or annealing process.[6] Contrarily, films deposited at low temperature in common exhibit poor capacities.[7] Thus, challenges remain to develop a favorable method to shun these processing constraints. A small number of recent articles have shown that the oxygen plasma treatment (PT) might be useful to minimize the oxygen-related defects at lower temperatures.[8] It is observed that leakage current density and the dielectric breakdown performance can be improved by using the plasma treatment in combination with lower temperature treatment. The electrical qualities of such films can be enhanced significantly after O_2 PT. However, it is still unclear how the oxygen plasma treatment is improving the stoichiometric and Si/ZrO_2 interfacial properties.

In the present work, we have fabricated low-temperature sol–gel spin-coated and O_2 plasma

(Received July 17, 2017; accepted November 7, 2017; published online November 20, 2017)

treated ZrO_2 thin film–based Metal–Insulator–Semiconductor (MIS) devices. To understand the influence of plasma treatment on the Si/ZrO_2 interface, deep level transient spectroscopy (DLTS) measurements were performed.

EXPERIMENTAL

The zirconia films were deposited by the facile spin-coating technique. Prior to the ZrO_2 film deposition, the plasma treatment on the Si wafer was done in an oxygen environment for 20 min at 0.008 mbar (Harrick Scientific Corp.). We have fabricated two sets of devices for comparison purposes, one is only annealed at 350°C for 1 h (untreated) and other is treated with O_2 plasma for 5 min, followed by annealing at 350°C for 1 h under the ambient conditions. Mmore information about the device fabrication process can be found in our previous work.[9] The plasma treated and untreated films were then integrated in a MIS structure to perform the electrical analysis. The Aluminum (Al) metal was thermally evaporated to a thickness of 150 nm using a metal mask with a circular hole (d = 288 μm) on the samples as a top gate electrode. The capacitance–voltage (CV) and current–voltage (JV) characteristics were recorded using a B1500A Semiconductor Device Parameter Analyzer. For the DLTS measurements, the devices were mounted on T05 headers. The measurements were performed at temperatures ranging from 100 K to 375 K in a liquid nitrogen cryostat. The details of DLTS setup and theory have been given in our earlier work.[6,10]

RESULTS AND DISCUSSION

The CV plot of the devices fabricated in this study with and without plasma treatment is shown in Fig. 1a. The schematic diagram of the device is given as the inset to Fig. 1a. Cross-sectional scanning electron microscope (SEM) images were used to measure the zirconia film thickness, and the experimental and Cauchy model fitted ellipsometery data (ψ–Δ–λ) to verify the thickness measured by cross-sectional SEM are given in Fig. 1b and c, respectively. The thickness extracted by both methods is in close agreement within the margin of error of the measurements. The thickness of the ZrO_2 film was found $\sim$ 35 nm. The plasma treated CV curve shows the proper accumulation, depletion, and inversion regions with a negligible hysteresis. The flat band voltage (V_{FB}) shifted to $-$ 0.9 V from 0.5 V and oxide trapped charges (Q_{ot}) diminished from 1.12×10^{12} cm^{-2} to 5.1×10^{10} cm^{-2} after PT. The dielectric constant (κ) estimated from accumulation capacitance of the device using Eq. 1[11] was found to be 18 in both the cases.

$$k = \frac{C_{ox} t_{ox}}{\varepsilon_0 A}, \tag{1}$$

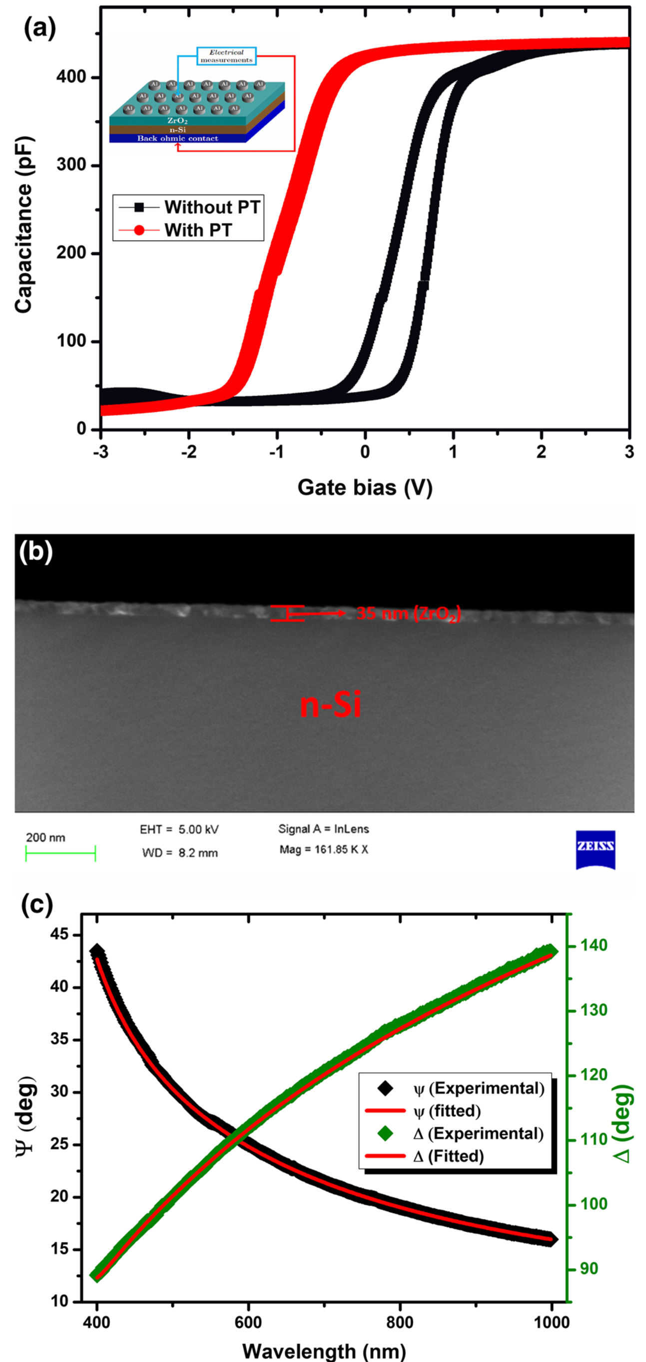

Fig. 1. (a) The capacitance–voltage characteristics of Al/ZrO_2/n-Si MIS structure without and with plasma treatment (PT). Inset shows the schematic diagram of the device. The PT improves the CV curve. (b) The cross-sectional SEM image of the ZrO_2 film on Si for the thickness estimation. (c) The ellipsometery data (ψ–Δ–λ) for the verification of thickness analysis.

where, C_{ox}, t_{ox}, ε_0 and A are the accumulation capacitance, thickness of the ZrO_2 film, permittivity of free space, and area of the top gate electrode of the MIS devices, respectively.

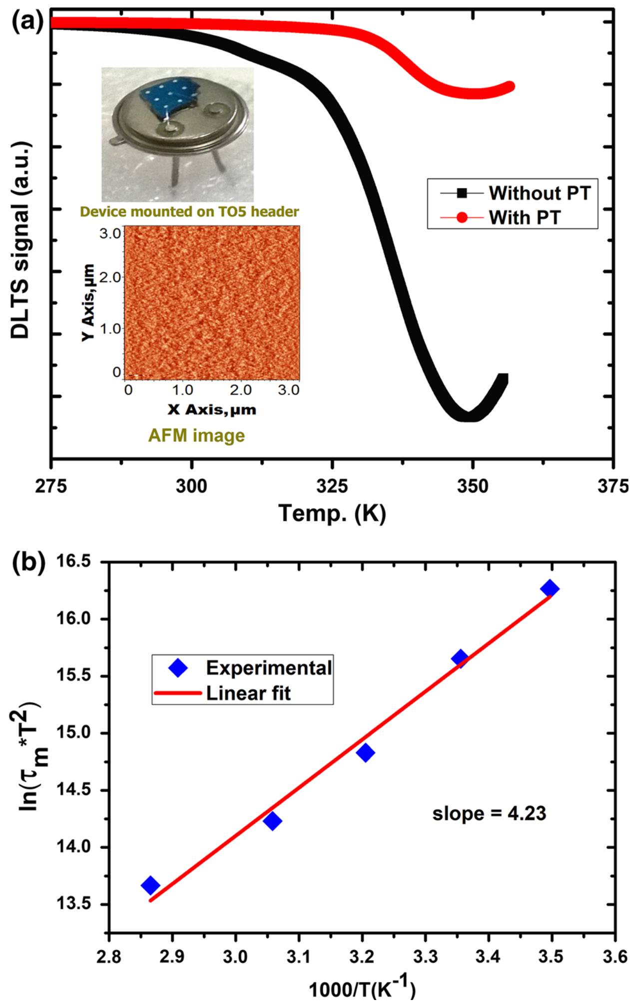

Fig. 2. (a) DLTS spectra of the Al/ZrO_2/n-Si MIS devices without and with plasma treatment (PT). Inset shows the image of the device mounted on a TO5 header for DLTS measurements. The D_{it} estimated with single shot DLTS is indicting the reduction of interface state density after PT. The RMS surface roughness was achieved 0.2 nm. (b) Arrhenius plot of Al/ZrO_2/Si MIS device extracted from DLTS spectra.

Figure 2a shows the DLTS spectra of the plasma treated and untreated devices. The quiescent and pulse voltage for the DLTS measurement were chosen according to CV plot as -2 and 2.5 V, respectively. We have selected a filling pulse such that our device should oscillate between depletion to accumulation region and interface traps should get charged and discharged.[10] The transient is recorded as a function of temperature and enclosed the information about the interface states density (D_{it}). The pulse width (t_p) was taken sufficiently large, 10 ms, such that all traps get filled during the DLTS operation. The DLTS spectra observed is probably due to the creation of minority carriers in the depletion region or in the neutral region in a MIS structure.[12,13]

The D_{it} is extracted from the DLTS spectra (Fig. 2a) using Eq. 2 as it is reported previously.[6,14]

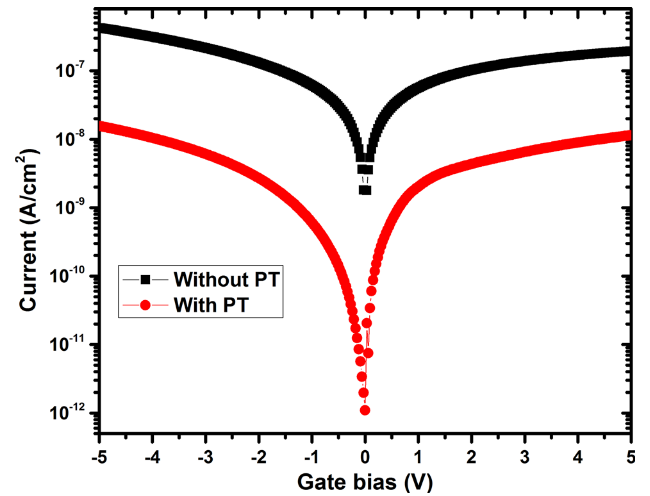

Fig. 3. The JV characteristics of untreated and plasma treated Al/ZrO_2/n-Si MIS devices. Plasma treated films shows an improved leakage current density as compared to an untreated one.

$$D_{it} = \frac{\varepsilon_{si} C_{ox} N_D \Delta C_{max}}{C_0^3 kT \ln(t_2/t_1)}, \qquad (2)$$

where 'ε_{si}' is the permittivity of Si, C_{ox} is the accumulation capacitance, N_D is the donor doping concentration, ΔC is the maximum DLTS signal, C_o is the depletion capacitance, and T is the DLTS peak temperature in K.

It has been observed that D_{it} reduces from 4×10^{11} eV^{-1} cm^{-2} to 7.1×10^{10} eV^{-1} cm^{-2} after plasma treatment, and this is attributed to the passivation of oxygen vacancies near the Si/ZrO_2 interface. Moreover, theoretical studies have suggested the accumulation of oxygen vacancies near the Si/high-k interface.[15] It is understood that numerous oxygen ions and radicals, such as O^+, O^- and O^{2+} are present in oxygen plasma and during the oxygen plasma exposure these are plausibly passivizing the oxygen vacancies related defects and improving the capacitive behaviors of the films.[8]

To find out the energy level position of interfacial traps, an Arrhenius plot has been derived by repeating the DLTS temperature scan for different rate windows (t_w) and which is shown in Fig. 2b. The location of the trap energy level is 0.36 eV below the conduction band edge and this is similar to interfacial trap position reported by Zhan et al.[16] for the HfAlO/Si stack.

The inset to Fig. 2a displays the MIS devices on the TO5 header (for DLTS measurements) and Atomic Force microscopy (AFM) image of the zirconia films. The surface topography of the plasma treated zirconia film is measured by AFM and RMS surface roughness and was found to be 0.2 nm. This quite smooth surface is beneficial towards their integration in TFTs.

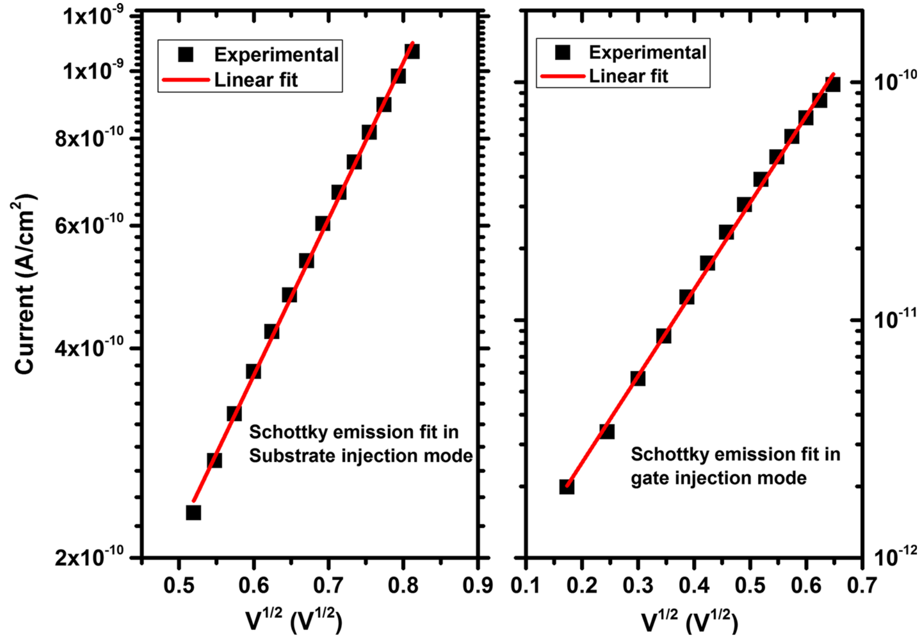

Fig. 4. Schottky emission (SE) regions for the gate and substrate injection mode to estimate the barrier heights.

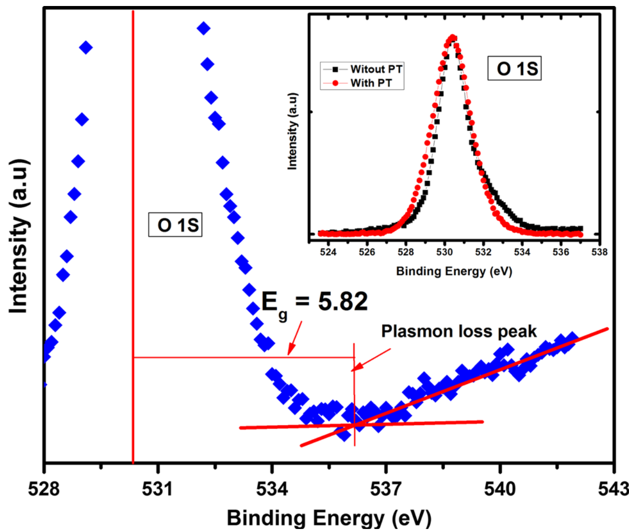

Fig. 5. The bandgap estimation of ZrO_2 films from the O1s Plasmon loss spectra. Inset shows O1s spectra of ZrO_2/Si without and with plasma treatment (PT). Disappearance of the shoulder peak suggests the reduction of oxygen vacancies after PT.

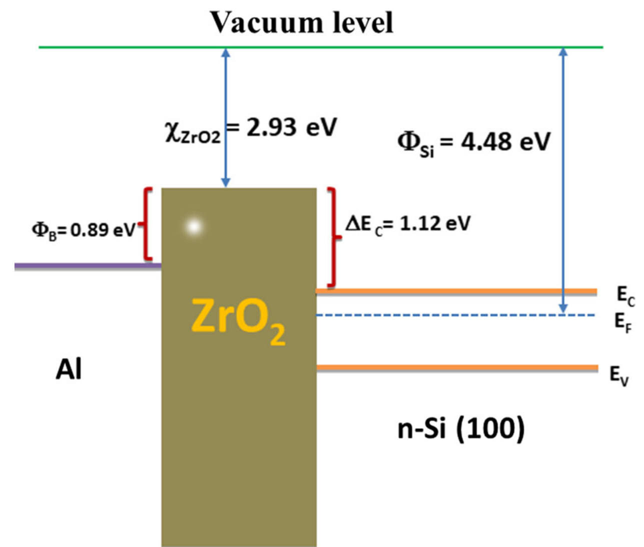

Fig. 6. Simplified band alignment of Al/ZrO_2/n-Si MIS device derived from the Schottky emission (SE) region of the JV characteristics.

The current conduction in a MIS stack is examined and found to disclose a bias dependence. The JV plot of the untreated and plasma treated films is shown in Fig. 3. The untreated ZrO_2 film displayed poor leakage behavior due to the of several traps within the film and at the interface; O_2 plasma treated films show improved leakage current density as it has changed from 5.4×10^{-8} A/cm^2 to 1.98×10^{-9} A/cm^2 for the gate injection mode and 6.4×10^{-8} A/cm^2 to 6.3×10^{-10}A/cm^2 for the substrate injection mode at 1 V. Again, the PT suppresses the oxygen-related defects.[8,17] Schottky emission (SE) is dominating at small biases, while other conduction mechanisms such as; PF, FN tunneling, and SCLC are dominating at intermediate and higher biasing conditions, respectively. We have calculated the Al/ZrO_2 and ZrO_2/Si barrier heights by fitting the Schottky emission (Eq. 3) as shown in Fig. 4. Later from this, the conduction band offset and electron affinity of zZircoina films were estimated.

Table I. Technology comparison with present work

Fabrication technique	κ	T_a (°C)	J@1 V (A cm^{-2})	References
PECVD	15	700	1×10^{-7}	Ref. 8
Sputtering	18	500	2×10^{-7}	Ref. 9
Spin-coating	7	700	4.7×10^{-7}	Ref. 10
Spin-coating and plasma treated	18	350	6.3×10^{-10}	[*]

κ—Dielectric constant, J—leakage current, T_a—annealing temperature, *—present work.

$$J_{SE} = A^{*}T^{2}\exp\left[-\frac{q(\Phi_B - \sqrt{qE/4\pi\varepsilon_0\varepsilon_r})}{kT}\right], \quad (3)$$

where $A^{*} = 120\ (m^{*}_{ox}/m_0)$ (A/cm^2 K^2) is the Richardson constant, J, E, Φ_B, k, and T is current density, electric field, barrier height, Boltzmann constant, and absolute temperature, respectively.

The conduction band offset (barrier height of ZrO_2/Si) and Al/ZrO_2 barrier heights have been enhanced from 0.88 eV and 0.89 eV to 1.03 eV and 1.12 eV after PT. This can be understood as barrier heights are influenced by the PT. The formation of dipoles and removal of the oxygen vacancies are the main source of the variation.[18,19]

The band gap (E_g) of ZrO_2 film is estimated by performing a core level x-ray photoelectron spectroscopy (XPS) scan usually used for stoichiometric analysis. The E_g of the zirconia films was extracted using the inelastic loss spectrum of the core level electrons.[20] This was done to derive the band alignment of the Al/ZrO_2/Si stack, which is particularly important to study any gate stack with a high-k layer.[5] The sample geometry was ZrO_2 film on the silicon. As we know during the XPS measurement, insulating films may accumulate charges on the surface;, hence, to minimize this effect, aluminum thin film was deposited on the corner of the film and grounded to the sample holder. The surface of the film was cleaned by etching with the Ar^{+} ion beam prior to XPS measurements. The XPS measurement was performed using an AXIS ULTRA instrument with Al K-radiation (9 mA, 13 keV, 1486.6 eV, pass energy $\sim$ 130 eV, absolute resolution, and step size of 1 eV) in ultra-high vacuum conditions. Figure 5 shows the energy difference of the elastic peak (e.g., oxygen core level peak—$E_{O\ 1s}$) and the onset of inelastic losses (E_{loss}) which is equal to the band gap of zirconia films.[20,21] The band gap of zirconia is deduced to be 5.82 eV and in close agreement with previous reports.[22] The inset of Fig. 5 shows the O 1s core level spectra of untreated and treated zirconia films. The disappearance of the shoulder peak for the PT zirconia film suggests the reduction of oxygen vacancies inside the ZrO_2 films which have helped to improve the leakage current density.[23]

The band alignment of plasma treated MIS structure is derived by using barrier heights obtained from the Schottky emission and band gap of zirconia films derived from the Plasmon loss spectra. Figure 6 represents the simplified band alignment of a plasma treated Al/ZrO_2/n-Si MIS device. The technology comparison to the present work is given in Table I.[24–26] Hence, it is understood that interface engineering is possible by using suitable plasma treatment which can also help to reduce the high temperature post deposition annealing.

CONCLUSIONS

It is reported that the interface state density (D_{it}) reduces from 4×10^{11} eV^{-1} cm to 7.1×10^{10} eV^{-1} cm^{-2}, after plasma treatment; a five time reduction in D_{it} can be attributed to the passivation of oxygen vacancies near the Si/ZrO_2 interface, as they try to relocate near the interface. The untreated ZrO_2 film displayed poor leakage behavior due to the presence of several traps within the film and at the interface; O_2 plasma treated films shows improved leakage current density as it has been reduced from 5.4×10^{-8} A/cm^2 to 1.98×10^{-9} A/cm^2 for the gate injection mode and 6.4×10^{-8} A/cm^2 to 6.3×10^{-10} A/cm^2 for the substrate injection mode at 1 V. Hence, we suggest that the plasma treatment might be useful in future device fabrication technology and the interface engineering is possible by using suitable plasma treatment, which can also help to reduce the high temperature post deposition annealing.

ACKNOWLEDGEMENTS

The authors acknowledge Prof. V. Venkataraman, Department of Physics, IISc, Bangalore and CeNSE, IISc, Bangalore for experimental facilities.

REFERENCES

1. A. Javey, H. Kim, M. Brink, Q. Wang, A. Ural, J. Guo, P. McIntyre, P. McEuen, M. Lundstrom, and H. Dai, *Nat. Mat.* 1, 241 (2002).
2. E.S. Shin, J.D. Oh, D.K. Kim, Y.-G. Ha, and J.H. Choi, *J. Phys. D Appl. Phys.* 48, 45105 (2015).
3. J.H. Park, J.Y. Oh, S.W. Han, and T. Il, Lee, and H.K. Baik. *ACS Appl. Mater. Interfaces* 7, 4494 (2015).
4. Y. Su, C. Wang, W. Xie, F. Xie, J. Chen, N. Zhao, and J. Xu, *A.C.S. Appl. Mater. Interfaces* 3, 4662 (2011).

5. A. Kumar, S. Mondal, and K.S.R. Koteswara Rao, *J. Appl. Phys.* 121, 85301 (2017).
6. A. Kumar, S. Mondal, and K.S.R. Koteswara Rao, *AIP Adv.* 5, 117122 (2015).
7. A. Kumar, S. Mondal, and K.S.R. Koteswara Rao, *J. Mater. Sci.: Mater. Electron.* 27, 5264 (2016).
8. J.S. Meena, M.C. Chu, S.W. Kuo, F.C. Chang, and F.H. Ko, *Phys. Chem. Chem. Phys.* 12, 2582 (2010).
9. A. Kumar, S. Mondal, and K.S.R. Koteswara Rao, *Appl. Surf. Sci.* 370, 373 (2016).
10. A. Kumar, S. Mondal, and K.S.R. Koteswara Rao, *Appl. Phys. Lett.* 110, 132904 (2017).
11. S. Mondal and A. Kumar, *Superlatt. Microstruct.* 100, 876 (2016).
12. N.O. Pearce, B. Hamilton, A.R. Peaker, and R.A. Craven, *J. Appl. Phys.* 62, 576 (1987).
13. S.N. Volkos, E.S. Efthymiou, S. Bernardini, I.D. Hawkins, A.R. Peaker, and G. Petkos, *J. Appl. Phys.* 100, 124103 (2006).
14. S. Kundu, Y. Anitha, S. Chakraborty, and P. Banerji, *J. Vac. Sci. Technol. B* 30, 051206 (2012).
15. C. Tang and R. Ramprasad, *Appl. Phys. Lett.* 92, 182908 (2008).
16. N. Zhan, M. Xu, D. Wei, and F. Lu, *Appl. Surf. Sci.* 254, 7512 (2008).
17. J. Singh, M. Chu, C. Wu, J. Liang, and Y. Chang, *Org. Electron.* 13, 721 (2012).
18. Z.Q. Liu, W.K. Chim, S.Y. Chiam, J.S. Pan, and C.M. Ng, *J. Mater. Chem.* 22, 17887 (2012).
19. L. Giordano, F. Cinquini, and G. Pacchioni, *Phys. Rev. B* 73, 45414 (2006).
20. A. Kumar, S. Mondal, and K.S.R. Koteswara Rao, *Appl. Phys. A* 122, 11 (2016).
21. M.T. Nichols, W. Li, and D. Pei, G. a. Antonelli, Q. Lin, S. Banna, Y. Nishi, and J.L. Shohet. *J. Appl. Phys.* 115, 94105 (2014).
22. J.H. Park, Y.B. Yoo, K.H. Lee, W.S. Jang, J.Y. Oh, S.S. Chae, andH.K. Baik, *ACS Appl. Mater. Interfaces* 5, 410 (2012).
23. K.L. Ganapathi, N. Bhat, and S. Mohan, *Appl. Phys. Lett.* 103, 1 (2013).
24. J. Liu, M. Liao, M. Imura, A. Tanaka, H. Iwai, and Y. Koide, *Sci. Rep.* 4, 6395 (2014).
25. F.-C. Chiu, Z.H. Lin, C.-W. Chang, C.-C. Wang, K.-F. Chuang, C.Y. Huang, J.Y. Lee, and H.-L. Hwang, *J. Appl. Phys.* 97, 34506 (2005).
26. S. Dutta, A. Pandey, I. Yadav, O.P. Thakur, A. Kumar, R. Pal, and R. Chatterjee, *J. Appl. Phys.* 114, 14105 (2013).